Electrohydrodynamic Properties of Succinoglycan as Probed by Fluorescence Correlation Spectroscopy, Potentiometric Titration and Capillary Electrophoresis

Jérôme F. L. Duval,*[,†,‡] Vera I. Slaveykova,[§] Monika Hosse,[†] Jacques Buffle,[†] and Kevin J. Wilkinson[||]

CABE (Analytical and Biophysical Environmental Chemistry), University of Geneva, Sciences II, 30 Quai E. Ansermet, 1211 Geneva 4, Switzerland, Environmental Biophysical Chemistry Group GE−ISTE−ENAC, Ecole Polytechnique Fédérale de Lausanne, Station 2, Lausanne, CH-1015, Switzerland, and Department of Chemistry, University of Montreal, C.P. 6128, succursale Centre-ville, Montréal, Canada H3C 3J7

Received April 9, 2006; Revised Manuscript Received July 17, 2006

The electrostatic, hydrodynamic and conformational properties of aqueous solutions of succinoglycan have been analyzed by fluorescence correlation spectroscopy (FCS), proton titration, and capillary electrophoresis (CE) over a large range of pH values and electrolyte (NaCl) concentrations. Using the theoretical formalism developed previously for the electrokinetic properties of soft, permeable particles, a quantitative analysis for the electrohydrodynamics of succinoglycan is performed by taking into account, in a self-consistent manner, the measured values of the diffusion coefficients, electric charge densities, and electrophoretic mobilities. For that purpose, two limiting conformations for the polysaccharide in solution are tested, i.e. succinoglycan behaves as (i) a spherical, random coil polymer or (ii) a rodlike particle with charged lateral chains. The results show that satisfactory modeling of the titration data for ionic strengths larger than 50 mM can be accomplished using both geometries over the entire range of pH values. Electrophoretic mobilities measured for sufficiently large pH values (pH > 5−6) are in line with predictions based on either model. The best manner to discriminate between these two conceptual models is briefly discussed. For low pH values (pH < 5), both models indicate aggregation, resulting in an increase of the hydrodynamic permeability and a decrease of the diffusion coefficient.

1. Introduction

Succinoglycan is an anionic extracellular polysaccharide,[1] produced by bacteria of the species *Pseudomonas*, *Rhizobium*, *Agrobacterium*, and *Alcaligenes*.[2,3] It has been shown that, on average, its repeating unit is composed of a 7:1:1:1 D-glucose:D-galactose:pyruvate:succinate ratio.[3] The macromolecular properties, in particular, the conformations of this biopolymer, are strongly mediated by the temperature, pH, and ionic strength of the neighboring solution[3,4] in addition to the origin and/or method of isolation and purification of the biopolymer.[5] Previous studies have indicated that succinoglycan is a single extended chain in aqueous solutions in the absence of salt,[6,7] whereas a transition from a stretched to a single helical chain has been observed with increasing ionic strength.[3,4,8] Using atomic force microscopy, Balnois et al.[1] showed that adsorbed succinoglycan existed as a mixture of flexible, individual chains and rigid dimers in pure water whereas only semirigid individual chains were observed in 0.01 M KCl. Upon increase of the ionic strength, the individual chains were shown to form a gel-network like structure.

The conformations of the polysaccharide, its flexibility, size, and electric charge play key roles in its function. Variations in ionic strength, pH, or polymer concentration are important parameters that are likely to induce significant structural modifications as a result of the accompanying changes in the inter- and/or intramolecular forces. To date, the biopolymer structure has been mainly probed with static and dynamic light scattering, differential scanning calorimetry, viscosity, optical rotation measurements, or atomic force microscopy.[1−5] To the best of our knowledge, little attention has been devoted to examining the adequacy of the electrokinetic methods, including electrophoresis, to address the physicochemical properties of succinoglycan. These methods, however, are known to be extremely sensitive to variations of the density of the electric charge carried by the macromolecule,[9] the molecular geometry, structural arrangement, hydrodynamic permeability, and size.[10−13]

This paper was designed to investigate the electrostatic and hydrodynamic character of succinoglycan on the basis of electrophoretic mobility measurements performed by capillary electrophoresis (CE) over a large range of pH and ionic strengths in aqueous medium. These features are intrinsically related to the conformational characteristics of the macromolecule. Analysis was refined by the independent evaluation of the electric charge density and size of the succinoglycan using potentiometric titration and fluorescence correlation spectroscopy (FCS). Both CE and FCS use laser-based detection systems so that, in theory, single molecule detection is possible. In practice, FCS allows the determination of diffusion coefficients for biopolymers at extremely low concentrations (near single molecule). The experimental results were interpreted on the basis of a recently developed theory for the electrophoresis of soft, hydrodynamically permeable, particles. Although the theory is available in the literature for soft, spherical particles,[12−14] the

* To whom correspondence should be addressed.
[†] University of Geneva.
[‡] Current address: Laboratory Environment and Mineralurgy, Nancy-University, CNRS, 15 avenue du Charmois, B.P. 40, 54501 Vandoeuvre-lès-Nancy Cedex, France.
[§] Ecole Polytechnique Fédérale de Lausanne.
[||] University of Montreal.

10.1021/bm060346n CCC: $33.50
Published on Web 09/12/2006

theory for soft, rodlike particles with charged lateral chains is described here for the first time. Mobility measurements were analyzed by numerical resolution of the governing transport and electrostatic equations, without any restriction on the charge of the macromolecule (inferred from titration measurements), its size (derived from FCS results), and the Debye layer thickness (determined from ionic strength). The merits of considering succinoglycan as a soft spherical particle or as a soft, rodlike particle, within the confines of electrophoretic theory, are quantitatively discussed in relationship with the known features of succinoglycan, as reported in the literature.

2. Experimental Section

2.1. Materials. A solution of 400 mg L^{-1} pre-sonicated succinoglycan, produced and purified as described in ref 2, was dissolved in MilliQ water, stirred for 12 h at room temperature, and then heated to 80 °C for 15 min in order to dissociate aggregated materials. Solutions were further filtered using a 0.22 μm Millipore filter. Two different series of polysaccharide solutions were prepared. First, succinoglycan solutions were prepared in carbonate buffer (pH = 10.3), and the ionic strength was varied from 5 to 400 mM by adding the appropriate amounts of $NaNO_3$. Second, solutions of constant ionic strength (5 mM $NaNO_3$) but different pH were prepared. The pH was kept constant during electrophoresis measurements by employing the sodium salts of several buffer solutions (Sigma or Fluka): acetate (pH = 4); 2-[*N*-morpholino]ethanesulfonic acid (MES, pH = 5.5 and 6.0); *N*,*N*-bis(2-hydroxyethyl)-2-aminoethansulfonic acid (BES, pH = 7.0 and 8.0); 3-[(1,1-dimethyl-2-hydroxyethyl)amino]-2-hydroxypropanesulfonic acid) (AMPSO, pH = 8.0 and 9.0); and carbonate (pH = 10.0). Adjustments of pH were made with analytical grade hydrochloric acid and carefully measured with a digital pH meter (Metrohm Herisau).

2.2. Methods. 2.2.1. Fluorescence Correlation Spectroscopy (FCS). FCS measurements were carried out with a Zeiss Confocor Axiovert 135TV (Carl Zeiss) using an argon ion laser for fluorescence excitation at 488 nm. A detailed description of the technique is given elsewhere.[15] Results are the means of duplicate runs performed on different days using freshly prepared samples of 10−20 mg L^{-1}, depending on the signal intensity. Calibration of the FCS confocal volume was performed with rhodamine 6G (R6G), which has a known diffusion coefficient of 2.8×10^{-6} cm^2 s^{-1}.[16] Each run is the mean of 10 FCS measurements, each with an accumulation time of 100 s. Standard deviations were evaluated from duplicate runs rather than replicate measurements in a single run.

For FCS measurements, succinoglycan was labeled using a rhodamine derivative (R6113) that was covalently bound to the reducing end of the polysaccharide.[17] Solutions of the labeled succinoglycan were stored at 4 °C when not being used. Prior to use, solutions of the labeled succinoglycan were heated at 80 °C for 15 min to remove potential aggregates. A constant (small) amount of labeled succinoglycan was added to solutions of unlabeled succinoglycan for determinations of diffusion coefficients by FCS under the same pH and ionic strength conditions as employed for the electrokinetic and potentiometric titration measurements.

Diffusion coefficients of succinoglycan, denoted as D, were estimated from the measured diffusion times, τ, according to

$$D = \frac{\omega_{xy}^{\,2}}{4\tau} \tag{1}$$

where ω_{xy} is the transversal radius of the confocal volume.

2.2.2. Potentiometric Titrations. A total of 34 mL of 318 mg L^{-1} succinoglycan was titrated with 1 M HNO_3 and 1 M NaOH solutions (Metrohm Dosimats) in a thermostated titration cell (25 °C). Titrations were performed under N_2 atmosphere using CO_2-free NaOH. Initial ionic strengths of 0.05 and 0.1 M were adjusted by the addition of $NaNO_3$. The pH was monitored with duplicate pH electrodes (Metrohm) and a Ag/AgCl reference electrode (Metrohm) following calibration with standard buffer solutions of pH 4.0, 7.0, and 9.0. Potential measurements were recorded when the rate of the linear drift was less than 0.05 mV min^{-1}. For the data analysis, the ionic strength was calculated taking into account both the background electrolyte and the free $[H^+]$ and $[OH^-]$. Blank titrations of the background electrolyte were performed and subtracted from titration curves measured in the presence of succinoglycan.

2.2.3. Capillary Electrophoresis (CE). CE experiments were performed with a Beckman P/ACE 2100 instrument using an argon ion laser at 488 nm and 20−30 mW power, depending on the concentration of the analyte (1 g L^{-1} of succinoglycan). Fused-silica capillaries (100 μm internal diameter and 47 or 57 cm total length) were obtained from Composite Metal Services Ltd. Anodic injection and cathodic detection were employed using an applied potential of 28 kV for the pH studies and 3 kV for the ionic strength studies. The temperature was maintained at 25 °C. Data outside the linear range of an Ohm's plot were discarded. A 10 s hydrostatic pressure injection, corresponding to a sample volume of ca. 180 nL, was used. Prior to sample injection, capillaries were washed with 0.1 M NaOH for 1 min and with the running buffer for another minute. Results are the means of three replicate samples, which were run in variable order.

3. Theory

3.1. Size Determination of the Biomacromolecules. The effective hydrodynamic radius of a sphero-colloid, denoted as δ_H, can be estimated from its diffusion coefficient D, as measured by FCS, using the Stokes−Einstein equation

$$\delta_H = k_B T/6\pi\eta D \tag{2}$$

where k_B is the Boltzmann constant, T the absolute temperature, and η the dynamic viscosity of the medium. Equation 2 is strictly valid for hard, rigid spheres, but its use remains legitimate for spherical permeable particles (Figure 1) characterized by a typical flow penetration length that is significantly lower than δ_H. In addition, macromolecules must be in the dilute regime and interchain interactions must be neglected.[18,19]

The mandatory prerequisite for the quantitative determination of the size and relevant lengths for a polymer of a given conformation is the knowledge, a priori, of some of the aspects pertaining to its structure such as the persistence length, the end-to-end distance, or the total contour length. Depending on the magnitude of these parameters, different models may be applied. For polyelectrolyte chains, the wormlike chain model, based on the Kirkwood−Riseman treatment,[20] is satisfactory. This model is a hybrid between the three extreme forms of a polymer: rod, coil, and helix.[21] For rigid or semirigid, rodlike molecules, Broersma's relationship[22] in addition to the wormlike chain model can be used, whereas for flexible wormlike chains with a persistence length that is much lower than the total contour length, the formalism by Hearst is applicable.[23,24] Within the framework of our analysis, all calculations (Figure 1) were performed by assuming a cylindrical chain of length L_{ee} (end-

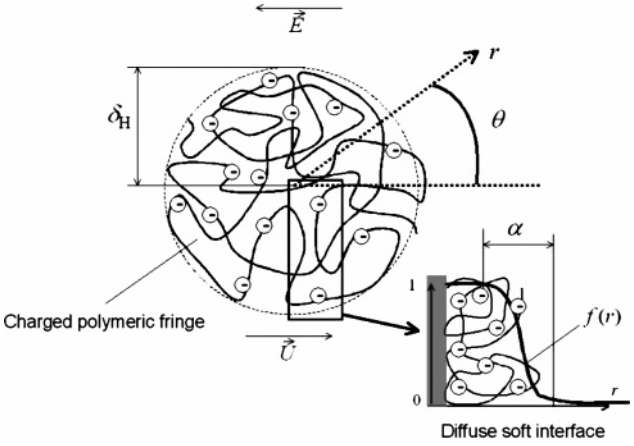

Figure 1. Schematic representation of a spherical diffuse soft particle, composed of a permeable, charged polyelectrolytic layer, moving with a velocity $\vec{U}$ in an electrolyte subjected to a dc electric field $\vec{E}$. The polar coordinate system (r,θ) is given. The origin for the r-axis is taken at the center of the particle. A graphical representation of the density distribution function f [30] is shown for the sake of completeness. When operating on the basis of a rodlike geometry, this schema relates to the cross section of the cylinder. The corresponding radius is called R_{pol}.

to-end distance), $L_{ee} \approx 467$ nm and radius $R_{pol} \approx 1$ nm. For the length L_{ee}, it is that calculated from a stretched molecule with length-normalized molar mass of 750 g mol^{-1} nm^{-1} [1,3] and a molar mass of 350 kg mol^{-1}.[25] It is in agreement with the end-to-end distance for rigid chains in water as measured by AFM.[1] For the radius, the value of $R_{pol} \approx 1$ nm corresponds well to the average height of a single rigid chain obtained by AFM.[1] Based upon the known chemical structure of succinoglycan,[3] it is also possible to estimate an end-to-end distance (or contour length for a stretched molecule) of 401 nm from the calculated monomer length of 1.9 nm and 211 repeat units per molecule.[26]

3.2. Modeling the Protolytic Properties of Succinoglycan. The amphoteric nature of the ionogenic sites distributed within the polymeric fringe of a soft particle (Figure 1) leads to a pH-dependence for the local space charge density that is denoted ρ_{fix}.[12] The charge measured by potentiometric titration, denoted as Q^o, is defined by the spatial integration of all local charges over the macromolecular volume, i.e.

$$Q^o = \int_V \rho_{fix}(\vec{r},\mathrm{pH})\, \mathrm{d}V \tag{3}$$

where V denotes the volume of the macromolecule and $\vec{r}$ is the vector position. The spatial dependence of ρ_{fix} is determined from (i) the local distribution of the protons within the macromolecule, which is in turn mediated by that of the electrostatic potential, denoted as $\psi(\vec{r})$,[12] and (ii) the spatial distribution for the density of the charged polymer segments throughout the permeable layer, $f(\vec{r})$. The inhomogeneous nature of the charged polymer segments is an important feature of this representation of the diffuse interface.[27−28] The volumic charge density, $\Gamma°$, is obtained by dividing Q^o by the volume V. As such, $\Gamma°$ may be viewed as an average space charge density per macromolecule. Since the electrokinetic behavior of soft particles depends on space charge densities and not on the total amount of charges carried by the particle, we choose to report in the following the quantity $\Gamma°$ (or equivalently $\Gamma°/F$ with F the Faraday's number) when comparing experimental and theoretical protolytic data. For sufficiently large electrolyte concentrations, $\psi(\vec{r}) \rightarrow 0$ and Q^o will depend solely on the chemical component of the isotherm, i.e., the reaction constants, K_p, associated to the p proton exchange equilibria responsible for the molecular charge. Rigorous evaluation of (3) requires estimation of $\psi(\vec{r})$. The latter is computed on the basis of the nonlinear Poisson−Boltzmann equation

$$\nabla^2 y(\vec{r}) = -\frac{\kappa^2}{\sum_i z_i^2 c_i^\infty}\left\{\sum_i z_i c_i^\infty \exp[-z_i y(\vec{r})] + \frac{\rho_{fix}(\vec{r},\mathrm{pH})}{F}\right\} \tag{4}$$

where κ is the reciprocal Debye length and z_i and c_i^∞ are the number of charges and bulk concentrations of the ionic species present in the electrolyte. The term $y(\vec{r})$ represents the dimensionless electrostatic potential, $y(\vec{r}) = F\psi(\vec{r})/RT$, where R is the gas constant. The boundary conditions associated with eq 4 are

$$y(\vec{r} \rightarrow \infty) = 0 \tag{5}$$

which defines the choice for the reference potential, and another condition specifies the value of the electric field at the center of the macromolecule ($\vec{r} = \vec{0}$), that is:

$$\nabla y(\vec{r})|_{\vec{r}=\vec{0}} = \vec{0} \tag{6}$$

The theoretical interpretation of titration measurements requires the evaluation of $\Gamma°$ as a function of pH and ionic strength via the nonlinear and coupled eqs 3 and 4−6. This is done according to an iterative scheme that is now described. As a starting point, the chemical component of $\Gamma°$ (as obtained for $\psi(\vec{r}) \rightarrow 0$, or equivalently $c_i^\infty \gg 1$) is represented by a Langmuir−Freundlich isotherm defined by

$$\Gamma^o(c_i^\infty \gg 1,\mathrm{pH}) = \rho_{fix}(c_i^\infty \gg 1,\mathrm{pH}) = \sum_p \Gamma^o_{max,p} \frac{1}{1 + 10^{m_p(\mathrm{p}K_p - \mathrm{pH})}} \tag{7}$$

where K_p is the median affinity parameters associated with the acido−basic equilibria of the ionogenic sites (p); the quantities $\Gamma^o_{max,p}$ are the maximum charge densities of the sites upon complete dissociation (i.e., for pH $\gg$ pK_p); m_p is the heterogeneity parameter of the sites, which determines the width of the distribution function for the corresponding affinity constant. For the sake of simplicity, we have assumed that the chains that extend from the molecule are homogeneous in space; that is, $f(\vec{r})$ corresponds to a step-function for eq 7. From the titration data measured for very large ionic strengths, the constants K_p, $\Gamma^o_{max,p}$, and m_p can easily be evaluated from the proton affinity spectrum as defined by the quantity $\mathrm{d}\Gamma°$ $(c_i^\infty \gg 1,\mathrm{pH})/\mathrm{dpH}$. Once K_p, $\Gamma^o_{max,p}$, and m_p are known, the local space charge density ρ_{fix} can be corrected by the appropriate Boltzmann factor to account for the local concentration of protons within the macromolecule such that

$$\rho_{fix}(c_i^\infty,\mathrm{pH}) = \sum_p \Gamma^o_{max,p} \frac{1}{1 + 10^{m_p(\mathrm{p}K_p - \mathrm{pH})} \exp[-m_p y(\vec{r})]} \tag{8}$$

After substitution of eq 8 in the nonlinear differential equation (eq 4), the potential distribution can be solved numerically for various ionic strengths using finite difference equations and a globally convergent Newton−Raphson algorithm.[29] The last step consists of integrating the local isotherms (eq 8) to estimate $\Gamma°$ or equivalently Q^o (eq 3). By merging experimental and theoretical data over the whole range of pH and ionic strengths,

K_p, $\Gamma^o_{max,p}$, and m_p can be optimized using a least-squares methodology. The impact of concentration gradients at the molecular interface (heterogeneous soft layer) on the titration data can be taken into account by appropriate choice of a prefactor $f(\vec{r})$ in eq 8.[30]

3.3. Modeling the Electrophoretic Mobilities of a Soft Macromolecule. The theory for the electrophoresis of a soft, spherical polyelectrolyte (Figure 1) has been discussed extensively elsewhere.[10,12−14,30] This approach was successful in the quantitative interpretation of the electro-hydrodynamic properties of bacteria[12] and a fulvic acid (molar mass of ca. 780 g mol^{-1}).[14] To the best of our knowledge, the detailed analysis for the electrophoretic migration of a rodlike permeable macromolecule under the action of a dc electric field has never been reported. In this section, the governing electrokinetic equations and the numerical computation are briefly described. This formalism extends that originally proposed by Ohshima, who derived approximate analytical expressions for the electrophoretic mobility of a soft, homogeneous, cylindrical particle for sufficiently large ionic strengths at which polarization and relaxation phenomena may be neglected (interfacial step-function modeling[11,31]). Analysis is performed here without any restriction on the macromolecular charge or ionic strength and may account for the heterogeneity of the extended polymer chains (diffuse interface modeling), if necessary.

Unlike for soft, spherical particles, the electrophoretic mobility, denoted as μ, for a cylindrical particle depends on the direction of its long axis as compared to that of the applied electric field. As is the case for hard cylinders, for a soft, cylindrical macromolecule that is oriented at an arbitrary angle between its axis and an applied field, μ is averaged, over a random distribution of orientations as follows:[32]

$$\mu = \frac{2}{3}\mu_{\perp} + \frac{1}{3}\mu_{\parallel} \tag{9}$$

where $\mu_{\perp}$ and $\mu_{\parallel}$ are the electrophoretic mobilities of the cylindrical particle with its axis perpendicular and parallel to the electric field, respectively.

3.3.1. Fundamental Equations for the Derivation of $\mu_{\perp}$. For an infinitely long cylindrical soft particle, i.e. $L_{ee} \gg R_{pol}$, moving with a velocity $\vec{U}$ in an applied electric field $\vec{E}$, it can be easily demonstrated that $\mu_{\perp}$, defined by $\mu_{\perp} = U/E$, is independent of L_{ee}. The origin of the cylindrical polar coordinate (r,θ) is set at the center of the particle (Figure 1).

By assuming a radial dependence for f, it is possible to show, based on symmetry considerations,[33] that the liquid velocity $\vec{u}(\vec{r})$ at the position $\vec{r}$ relative to the particle ($\vec{u}(\vec{r}) \to -\vec{U}$ as $r \to \infty$) may be written in the vectorial form

$$\vec{u}(\vec{r}) = \left(-\frac{h(r)}{r} E\cos\theta, \frac{dh(r)}{dr} E\sin\theta, 0\right) \tag{10}$$

where h is a function of r that satisfies the boundary condition

$$h(r \to \infty) \to \mu_{\perp} r \tag{11}$$

By modeling the friction exerted by the polymer segments on the fluid flow in terms of resistance centers, as has been done in the framework of the Debye Bueche theory,[34] it is possible to derive the function $h(r)$ from the general form of the Navier−Stokes equation. The mathematics is straightforward but tedious. After some arrangement, the result is given as

$$L_r\{L_r h(r)\} - \lambda_o^2 f(r) L_r h(r) - \lambda_o^2 \frac{df(r)}{dr}\frac{dh(r)}{dr} = -\frac{F}{\eta}\frac{1}{r}\frac{dy(r)}{dr}\sum_i c_i^{\infty} z_i^2 \exp\{-z_i y(r)\}\chi_i(r) \tag{12}$$

with L_r corresponding to the differential operator $L_r \equiv d^2/dr^2 + (1/r)(d/dr) - 1/r^2$.

The quantity λ_o is the so-called softness parameter of the charged layer.[10] $1/\lambda_o$ has a length dimension and characterizes the typical penetration length of flow within the polymeric layer. The radial functions $\chi_i(r)$ represent the local variation of the electrochemical potential of the ion i due to a polarization of the double layer by the externally applied field, $\vec{E}$. The functions $\chi_{i=1,...,N}(r)$ (N denotes the number of ion types present in the solution) are defined by the differential equations[31]

$$i = 1, ..., N: \; L_r\chi_i(r) = \frac{dy(r)}{dr}\left\{z_i\frac{d\chi_i(r)}{dr} - \frac{\xi_i}{e}\frac{h(r)}{r}\right\} \tag{13}$$

where ξ_i is the drag coefficient of an ion i given by $\xi_i = z_i^2 eF/\lambda_i^{\infty}$; λ_i^{∞} is the limiting conductance of the ion i and e is the elementary charge. Following the strategy adopted for spherical symmetry,[30] it is possible to show that the boundary conditions associated to the functions h and χ_i can be given by

$$h(r \to 0) = 0; \left.\frac{dh}{dr}\right|_{r=0} = 0 \tag{14ab}$$

$$\left.\frac{d^2h}{dr^2}\right|_{r\to\infty} = 0; \; r^2\left.\frac{d(h/r)}{dr}\right|_{r\to\infty} = 0 \tag{15ab}$$

$$i = 1, ..., N: \; \left.\frac{d\chi_i(r)}{dr}\right|_{r=0} = 0; \; \chi_i(r\to\infty) \to r \tag{16ab}$$

The potential $y(r)$ is computed on the basis of eq 4 with the boundary conditions (5−6).

The theoretical calculation of $\mu_{\perp}$ requires the consistent numerical evaluation of (a) the electroosmotic velocity profile $\vec{u}(\vec{r})$, or equivalently $h(r)$, as defined by eqs 12 and 14−15 (hydrodynamics), (b) the distribution of the local dimensionless equilibrium potential (electrostatics, eqs 4−6), and (c) the radial functions $\chi_{i=1,...,N}(r)$ (eqs 13 and 16). After a suitable change of variables, the set of coupled equations (12−16) may be transformed into a system of first-order differential equations with boundaries written in terms of explicit algebraic relations between the new variables. This multidimensional root-problem can then be solved by numerical shooting[29] from $r \gg \kappa^{-1}$ to the position $r = 0$ using an adaptive stepsize Runge−Kutta method of the fifth-order implemented with a Newton−Raphson type scheme.[29,35] The potential was evaluated on the self-controlled nonuniform grid by cubic interpolation of the results obtained from the finite difference algorithm with a uniform step size.

The main assumptions of the above formalism are (a) the Reynolds numbers of the liquid flow inside and outside the charged, soft polymeric layer are small so that the liquid may be regarded as incompressible; (b) the electrophoretic velocity, $\vec{U}$, is proportional to the applied field, $\vec{E}$, which is correct for low E (in electrophoresis of the first kind, as considered here, terms in E of order higher than 1 may be neglected); and (c) the relative permittivities, ϵ_r, inside and outside the polymeric layer are the same or, equivalently, the water content within the soft layer is sufficiently large to neglect any spatial gradients

in ϵ_r. These assumptions are in line with the conditions under which the electrophoretic experiments were carried out and in relationship to the nature of the macromolecules that were investigated.

3.3.2. Fundamental Equations for the Derivation of $\mu_{||}$. When the cylinder is oriented parallel to $\vec{E}$, the components of the flow velocity $\vec{u}(r)$, according to the unit vectors describing the cylindrical coordinate system (r,θ,z), are simply given by

$$\vec{u}(r) = \{0,0,u_z(r)\} \tag{17}$$

The Navier Stokes equation that determines $u_z(r)$ can be given as

$$\frac{1}{r}\frac{\mathrm{d}}{\mathrm{d}r}\left(r\frac{\mathrm{d}u_z(r)}{\mathrm{d}r}\right) - \lambda_o^2 f(r)u_z(r) - \frac{EF}{\eta}\sum_i z_i c_i^{\infty}\exp(-z_i y(r)) = 0 \tag{18}$$

where the function $f(r)$ is considered to be radial (as above) and the assumptions governing the validity of eq 18 are the same as those in the preceding section. $u_z(r)$ is limited by the boundaries

$$\left.\frac{\mathrm{d}u_z(r)}{\mathrm{d}r}\right|_{r\to 0} = 0;\ u_z(r\to\infty) = -\mu_{||}E \tag{19}$$

Computation of the hydrodynamic flow profile, $u_z(r)$, as determined by eqs 18 and 19 and evaluation of the associated $\mu_{||}$ may be performed using classical finite-differences schemes or a numerical algorithm very similar to that employed for the evaluation of $\mu_{\perp}$.

4. Results and Discussion

4.1. Analysis of the Electrohydrodynamics of Succinoglycan under the Assumption of a random, Spherical Coil. Diffusion coefficients were used to estimate hydrodynamic radii (section 3.1). Variations of the diffusion coefficients with pH and ionic strength were employed to follow conformational changes/aggregation of the macromolecules.[36] At pH = 10.3, diffusion coefficients remained nearly constant in the range 5−100 mM, whereas a slight, statistically significant, decrease was observed when the ionic strength was raised above 100 mM (Figure 2A). The decrease in D corresponded to an increase in the hydrodynamic radius δ_H (eq 2) from 10.8 to 12.7 nm. Given the error bar in the measurements, especially at large ionic strengths (see related comment below), this variation in D did not indicate a large conformational change or significant aggregation at pH = 10.3. The difficulty in performing FCS measurements at large ionic strengths is likely linked to changes in the refractive index of the solution resulting in a defocalization of the confocal volume. This problem was partially resolved by carrying out the calibration of the confocal volume using exactly the same ionic strengths as were used for the measurement of the diffusion coefficients.

At constant ionic strength, $I = 5$ mM, a significant decrease in D was observed with decreasing pH (Figure 2B). In this case, δ_H increased from 10.3 nm at high pH to 14.5 nm at low pH. This increase in δ_H is likely due to aggregation of succinoglycan, as resulting from the decrease of the intermolecular interactions following a decrease of the macromolecular charge.

Titration data performed at $I = 100$ and 50 mM (Figure 3A) were quantitatively interpreted following the theoretical schema outlined in section 3.2 (eqs 3−8). The conversion of the measured data (expressed in charge per unit mass) into a volumic charge density, Γ°, was carried out using $\delta_H = 10.8$ nm, in line with Figure 2A, and a molar mass of 350 kg mol^{-1}.[25] Excellent agreement between the theoretical predictions and experimental data was obtained over the whole range of examined pH. In the modeling, we considered two types of sites ($p = 1$ and 2), based upon the observation of two maxima in the proton affinity spectra. The characteristic values obtained for pK_p, m_p, and $\Gamma^{o}_{max,p}$ are reported in Table 1. The median intrinsic stability constant p$K_1 = 4.58$ is in fair agreement with the reported dissociation constants of succinic acid (p$K = 4.16$ (first step) and p$K = 5.66$ (second step)) and with a p$K = 2.9$ for the dissociation of the pyruvate groups. The relatively broad spectrum for the affinity constant pK_1 associated to the first peak (see m_1 value) makes it impossible to detect each of the three aforementioned proton exchange equilibria separately. The slight increase (in magnitude) of the measured volumic charge density above pH > 7 is reflected by the second type of sites (p$K_2 = 8.6$) for which the volumic concentration, $\Gamma^{o}_{max,p=2}$, is about 8 times lower than that for the sites $p = 1$. Ruling out the possibility of the deprotonation of hydroxyl groups that might only occur well above pH 10, this residual charge might be due to "impurities" in the polysaccharides incorporated during the bacterial production. An observed, pronounced chemical heterogeneity, reflected in the value of m_2, prevents us from drawing more firm conclusions. Titration data at very high and very low pH values were very much more scattered (and not reported), likely due to the hydrolysis of oxygen bridges along the succinoglycan chain.

As expected from classical double layer theory, at a given pH, the quantity of titrable charges increases with increasing ionic strength due to the screening of fixed charges. The difference among the titration data measured for various ionic

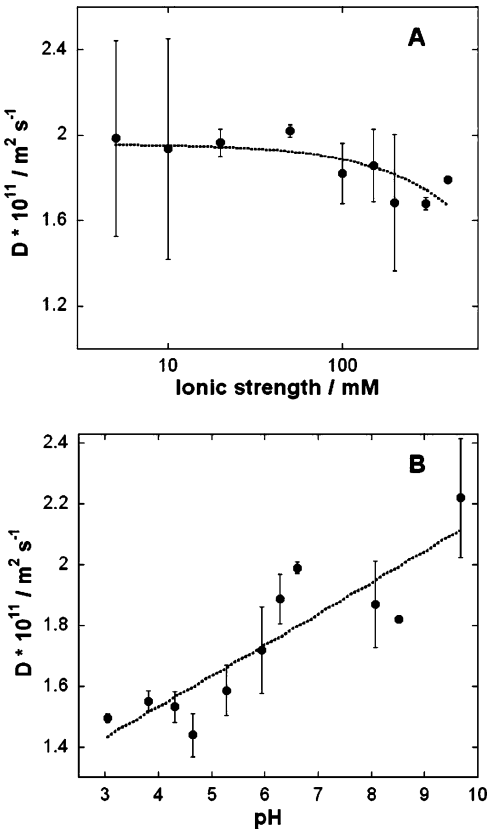

Figure 2. (A) Diffusion coefficient measured by FCS for succinoglycan at pH 10.3 as a function of the ionic strength (NaCl). (B) Diffusion coefficient measured by FCS for succinoglycan in 5 mM NaCl as a function of pH.

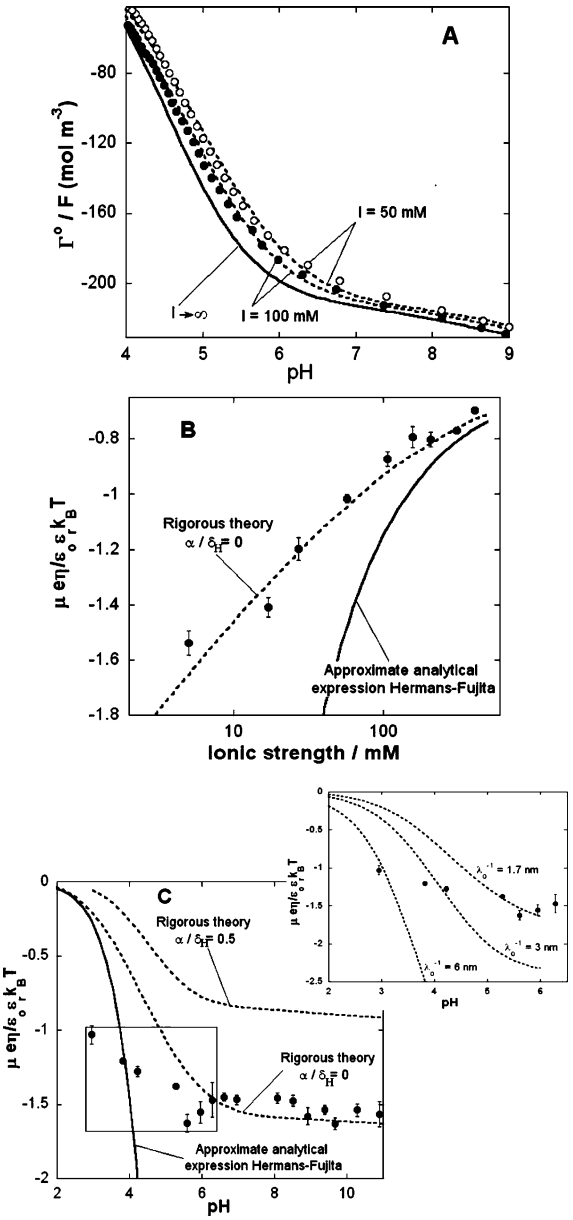

Figure 3. (A) Volumic charge density Γ° for succinoglycan viewed as a spherical polyelectrolyte as a function of pH for two ionic strengths (indicated). Points: experimental data; dashed curves: theoretical results obtained on the basis of the formalism given in section 3.2 using the parameters of Table 1. Size of the spherocolloid: $\delta_H = 10.8$ nm. (B) Dimensionless electrophoretic mobilities for succinoglycan as a function of (NaCl) ionic strength at pH 10.3 when the molecule is considered as a spherical polyelectrolyte. Points: experimental data; dashed curve: theoretical results obtained on the basis of the formalism of refs 12, 14, 30 with the parameters collected in Table 1 and $\delta_H = 10.8$ nm, $1/\lambda_o = 0.70$ nm, and $\alpha/\delta_H = 0$ (homogeneous distribution of the polymer segments within the macromolecule). The full line corresponds to predictions obtained with the approximate analytical expression of Hermans−Fujita.[39] In that case, the space charge density, i.e. ρ_o in refs 10, 39, has been replaced by the quantity Γ° ($I \rightarrow \infty$). (C) Dimensionless electrophoretic mobility for succinoglycan viewed as a spherical polelectrolyte as a function of pH in 5 mM NaCl. The model parameters and description of symbols are the same as in panel B. In the inset, theoretical mobilities (dashed curve) are depicted for $\delta_H = 14$ nm and various values of $1/\lambda_o$ (indicated). The other model parameters are those from Table 1 except for the $\Gamma^o_{max,p}$ that were evaluated so as to conserve the total amount of charges, i.e., $(\Gamma^o_{max,p}V)_{\delta H=14nm} = (\Gamma^o_{max,p}V)_{\delta H=10.8\ nm}$, where V is the volume of the macromolecule.

strengths is directly correlated to the magnitude of the local electrostatic potential distribution, as explained in section 3.2.

Table 1. Parameters Pertaining to the Protolytic Properties of Succinoglycan when Modeled as a Spherical Random, Coil Polymer

	$p = 1$	$p = 2$
m_p	0.81	0.62
pK_p	4.58	8.60
$\Gamma^o_{max,p}$ (mM)	−213	−26

The full line in Figure 3A describes the purely chemical (as opposed to columbic) component of the isotherm (eq 7), also called the master curve.

The methodology proposed in section 3.2 significantly improves the traditional Donnan approach that is often employed to account for proton (or metal) binding to organic macromolecules.[37,38] In this representation, no a priori assumptions are made on the potential distribution, which is numerically calculated using the nonlinear Poisson−Boltzmann equation. Indeed, the assumption of a Donnan potential within the macromolecule is not consistent with a local potential gradient (in particular at the interface with the aqueous medium) and is thus only correct for $\kappa\delta_H \gg 1$, i.e., questionable when operating at low ionic strength and/or with small molecules. Furthermore, fitting of the titration data with the Donnan model requires adjustment of the Donnan volumes, which do not always correspond to macromolecular sizes as measured by spectroscopic or other techniques.[38] The analysis presented here does not suffer from these limitations since it directly integrates size data obtained by FCS.

Using the measured protolytic properties and sizes of the succinoglycan, the measured electrophoretic mobility μ could be analyzed as a function of ionic strength at pH = 10.7 (Figure 3B)[12,14,30] with the hydrodynamic permeability $1/\lambda_o$ as the unique unknown variable. Very good agreement between theory and experiment was observed over the whole range of ionic strength 5 mM-400 mM with $1/\lambda_o \approx 0.70 \pm 0.02$ nm. The latter value corresponds to a fairly permeable particle ($\lambda_o\delta_H \approx 15$). It is noted that for large ionic strengths, the experimental mobility gradually reaches a finite, nonzero constant value, which is typical of a soft, charged polymer.[10,30] In contrast, the electrokinetic response for hard, i.e. impermeable, particles vanishes at large ionic strengths.[9] For the sake of comparison, results obtained using the approximate analytical expression derived by Hermans and Fujita[39] are also shown. Discrepancies between predictions based on rigorous theory and their expression become significant at lower ionic strengths, i.e., for higher local potentials $y(r)$, due to the fact that the analysis in ref 39 does not take polarization and relaxation of the double layer by the applied field into account (see ref 30 for further details). These phenomena are of prime importance for sufficiently large potentials,[40] as is the case for succinoglycan at pH = 10.3 ($\psi(r = 0) = -6$ mV/−135 mV for 500 mM/1 mM electrolyte). Modeling of the mobility data could be successfully performed using a homogeneous distribution of the polymer side chains, i.e., for $\alpha/\delta_H = 0$, where α is a typical decay length for the polymer concentration gradient at the interface (as represented by the function f introduced in Section 3). For an increasing α/δ_H, the interface becomes more and more diffuse.[30] The above mobility analysis demonstrates that if succinoglycan is treated as a charged, random coil polymer then its electrokinetic response at pH = 10.3 for varying I is solely determined by a charge (double layer) screening that excludes any structural changes to the molecule.

For a fixed ionic strength (5 mM NaCl), the pH dependency of the electrophoretic mobility is shown in Figure 3C. Theoreti-

cal predictions, based on the parameters of Table 1, i.e., $1/\lambda_o \approx 0.70$ nm (Figure 3B) and $\delta_H \approx 10.8$ nm (Figure 2B), are also reported. Between pH 6.5 and 11, μ remains constant and adopts a value that is in agreement with theory. In this pH range, the total volumic charge density is approximately constant (Figure 3A) because $\Gamma^o_{max,p=1} \gg \Gamma^o_{max,p=2}$ and the sites $p = 1$ are fully deprotonated. Below pH 6, the observed decrease in μ that originates from the protonation of pyruvate and succinate groups is qualitatively consistent with the decrease in $\Gamma°$. However, a stronger decrease in the electrophoretic mobilities was predicted by theory than was observed experimentally. Since significant increases of the hydrodynamic radii were measured by FCS with decreasing pH, we verified if the electrokinetic properties of succinoglycan at low pH could be performed by taking into account the appropriate δ_H values. For that purpose, mobility calculations were carried out with $\delta_H \approx 14$ nm, in agreement with the FCS results at low pH values (inset, Figure 3C). Data for pH < 6 could be fitted by considering an important variation of the penetration length ($1/\lambda_o$), ranging from 1.7 nm at pH = 6 to 6 nm at pH = 3. An increase in $1/\lambda_o$ corresponds to a reduction in electroosmotic drag, such that the electrophoretic mobility increases (in magnitude). For a decreasing pH, the moderate decrease in mobility cannot be quantitatively explained by an increase in molecular size and by the pH-dependence of $\Gamma°$. Nonetheless, indications from the FCS of a small amount of aggregation, may be sufficient to account for the observed strong variation in hydrodynamic properties, in particular $1/\lambda_o$. Qualitatively, the increased permeability that is observed with decreasing pH, i.e., decreasing intermolecular repulsion, can be understood by referring to the notion of hydrodynamic path. In the absence of aggregation processes (situation met for pH > 6 at 5 mM NaCl), the fluid flows within the macromolecules due to their soft nature. For an aggregate composed of several macromolecular entities (pH < 6), the fluid flow distribution is significantly perturbed since flow takes place not only through the permeable units, but also among them via (hydrodynamic) paths. As the number of units increases during aggregation, the number of hydrodynamic paths increases in parallel, as will the overall permeability. This feature is captured by an increase of the hydrodynamic penetration length, $1/\lambda_o$, with decreasing pH (see Figure 3C). Although the mobility analysis was performed by assuming that the aggregates maintained a spherical (or cylindrical, see section 4.2) symmetry which is necessarily an approximation, λ_o^{-1} can still be considered as an "effective" hydrodynamic penetration length. Similar results were found and discussed previously in our study of the electrokinetic features of humic acids.[14] For the sake of completeness, it can be seen (Figure 3C) that within the ranges of size, charge, and permeability that were investigated here, consideration of a diffuse distribution for the charged polymer segments within the macromolecule did not improve the fit for the mobility data at low pH values. Indeed, at given pH, when the diffuse character of the interface is increased, i.e., by increasing α/δ_H, the mobility decreases as the result of an increased electroosmotic drag.[30]

To summarize the preceding discussion, the representation of a succinoglycan as a random coil allowed for the quantitative interpretation of FCS, titration, and electrophoretic mobility measurements over a wide range of electrolyte concentrations (I = 5−400 mM) for pH > 6. Under those conditions, the magnitude of the electrophoretic mobility was primarily determined by the extent of charge screening by the ions in the electrical double layer. For pH < 6, partial aggregation must be taken into account in order to interpret the data. The aggregation results in significant modifications to the hydrodynamic and electrokinetic properties of the succinoglycan, as reflected in an increase of the softness degree with decreasing pH.

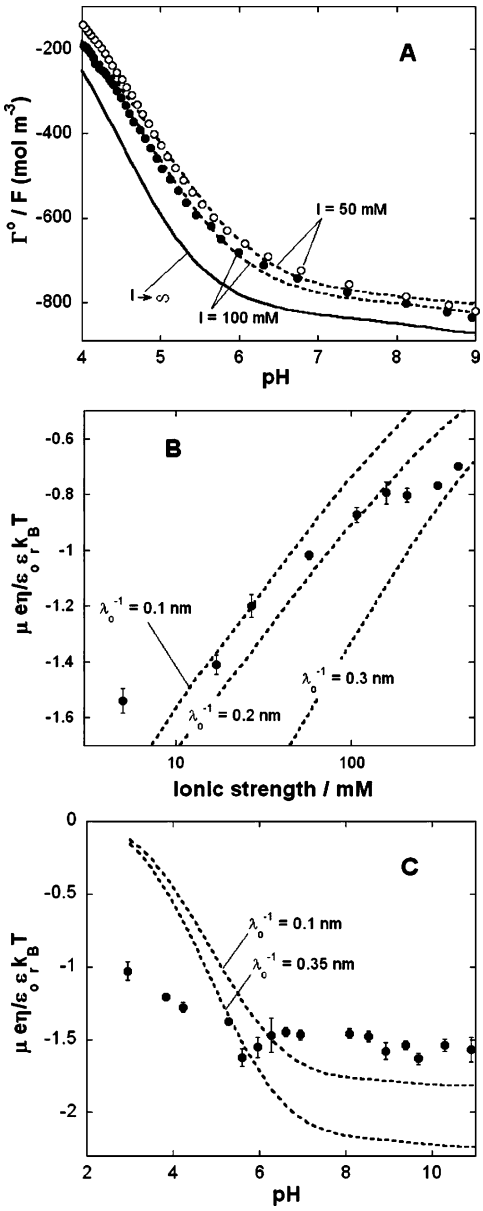

Figure 4. (A) Volumic charge density $\Gamma°$ for succinoglycan viewed as a polyelectrolytic, rodlike macromolecule as a function of pH for two (NaCl) ionic strengths. Points: experimental data. Dashed curves: theoretical results obtained on the basis of the formalism of section 3.2 with the parameters from Table 2. Size of the rodlike particle: $R_{pol} = 1$ nm, $L_{ee} = 467$ nm. (B) Dimensionless electrophoretic mobilities for succinoglycan viewed as a randomly oriented polyelectrolytic, rodlike molecule as a function of ionic strength at pH 10.3. Points: experimental data. Dashed curve: theoretical mobility μ (eq 9) obtained on the basis of the formalism of section 3.3 using the parameters collected in Table 2 and $\alpha/\delta_H = 0$ (homogeneous distribution of the polymer segments within the particle). The values of $1/\lambda_o$ are indicated. (C) As in panel B but the pH is varied and I = 5 mM.

4.2. Analysis of the Electrohydrodynamics of Succinoglycan under the Assumption of a Rodlike Geometry. Analysis of the titration data on the basis of the theory developed in section 3.2 for a rodlike geometry is reported in Figure 4A. In this case, using the parameters reported in Table 2, experimental data were satisfactorily described by theory over a broad range

Table 2. Parameters Describing the Protolytic Properties of Succinoglycan when Modeled as a Permeable Rodlike Macromolecule (Section 3.3)

	$p = 1$	$p = 2$
m_p	0.81	0.62
pK_p	4.48	8.60
$\Gamma^o_{max,p}$ (mM)	−829	−070

of pH values ($I = 50$ or 100 mM). Slight discrepancies were observed for pH < 4.5 and $I = 50$ mM. Due to volume variations for the spherical and cylindrical macromolecules, the corresponding concentrations of ionogenic sites, $\Gamma^o_{max,p}$, were different. As a general comment, $(\Gamma^\circ)_{sphere} < (\Gamma^\circ)_{cylinder}$ (in magnitude), so that, for a given pH and ionic strength, the electrostatic component of the proton adsorption isotherm is larger for a cylinder than for a sphere resulting in a larger shift of the master curve ($I \rightarrow \infty$) as compared to isotherms obtained at finite ionic strength.

Dimensionless electrophoretic mobilities (eq 9) were computed for hydrodynamic penetration lengths that varied between 0.1 and 0.3 nm ($R_{pol} = 1$ nm, see section 3.1; Figure 4B). The electrokinetic features of the "cylindrical" succinoglycan could not be reproduced over the entire range $I = 5-400$ mM using a unique value of $1/\lambda_o$. A similar observation was made for pH dependent mobility data at a fixed ionic strength ($I = 5$ mM, Figure 4C). Given the absence of changes to the diffusion coefficient for succinoglycan at pH 10.3 (Figure 2), no significant changes in the softness parameter could be expected due to variations in the ionic strength. The hypothesis of a randomly oriented charged cylindrical succinoglycan that is migrating under an applied electric field would appear to be inadequate to explain observed electrophoretic mobilities (Figure 4B,C).

Closer inspection of the parallel and perpendicular components of the mobility (sections 3.3.1 and 3.3.2) indicates that a value of $1/\lambda_o \approx 0.30-0.35$ nm is obtained from $\mu_\perp$ (pH 10.3, $I = 5-400$ mM; pH 6−10, $I = 5$ mM, Figure 5). Furthermore, below pH 6, data are consistent with the occurrence of aggregation, as reflected by an increase in $1/\lambda_o$ (section 4.1, Figure 3C) and the $\mu_{||}$ data. These conclusions are not qualitatively affected by variation of δ_H in the range 0.5−1.5 nm.

In the absence of aggregation, i.e., for pH > 6, the mobility data indicated that succinoglycan, if considered as rodlike, would remain perpendicular to the direction of the electric field during migration. This surprising observation might be explained by the fairly special chemical structure attributed to succinoglycan for which most of the molecular charge due to succinate functional groups is located along the short ($R_{pol} \ll L_c$), side chains of the macromolecule. In this case, the charge polarization and the associated dipoles should be much larger along the side chains than along the backbone of the macromolecule. Alignment of the dipoles according to the direction of the electric field, the most favorable situation from a thermodynamic point of view, would require the cylinder to position itself with its long axis perpendicular to the field. Although this result is consistent with the analysis of electrokinetic data, it implies that the corresponding gain in electrostatic energy would overcompensate for the loss of energy associated with the increased viscous forces resulting from an increased surface area exposed to fluid flow. Such a result would be expected only if the macromolecule exhibits a significant hydrodynamic penetration length, $1/\lambda_o$, as compared to its characteristic size, R_{pol}, as is the case for a rodlike succinoglycan ($\lambda_o R_{pol} \approx 3$). When lowering the pH, the charge carried by the succinoglycan decreases in magnitude, resulting in a decreased polarization of the side chains. Combination of this process with the formation of aggregates should in turn affect the orientation of the succinoglycan and lead to significant differences with the conformation adopted at larger pH values. This explanation is qualitatively consistent with the data in Figure 5B.

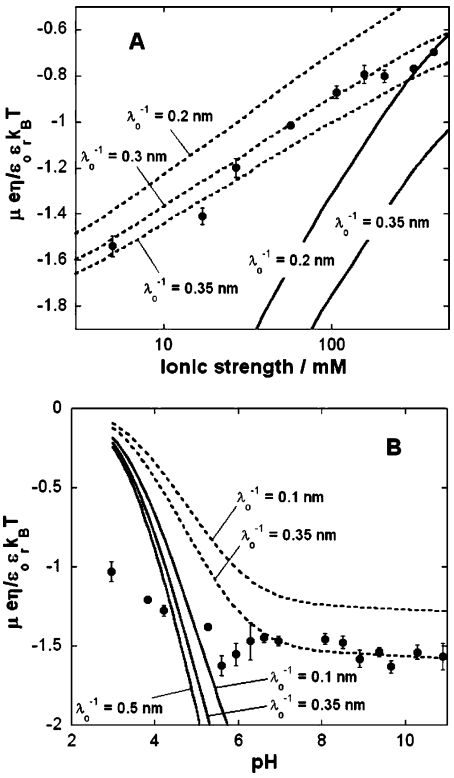

Figure 5. (A) Dimensionless electrophoretic mobilities for succinoglycan, viewed as a polyelectrolytic, rodlike molecule as a function of (NaCl) ionic strength at pH 10.3. Points: experimental data. Dashed curve: theoretical mobility $\mu_\perp$ (section 3.3.1). Full line curve: theoretical mobility $\mu_{||}$. Model parameters: see Table 2 and $\alpha/\delta_H = 0$ (homogeneous distribution of the polymer segments within the macromolecule). The values of $1/\lambda_o$ are indicated. (B) As in panel A but the pH is varied and $I = 5$ mM.

5. Conclusions

In sections 4.1 and 4.2, it was shown that the size, titration, and electrokinetic data collected above pH 6 could be quantitatively modeled by representing succinoglycan as either a random coil or a rodlike polymer. A more complex modeling of succinoglycan as a semiflexible molecule with a rigidity that varies as a function of the solution physicochemistry[1] was not possible. Nevertheless, the present results suggest that the charged macromolecule can move perpendicular to the direction of the electric field during migration. Results for the lower pH, i.e. values approaching and below the pK_a values, showed that aggregation of the succinoglycan is likely to occur, resulting in a significant decrease in the diffusion coefficient (40% decrease). For both extreme representations of the molecule (spherical coil or rigid rod), it could be concluded that permeability increased significantly at low pH but that this was likely due to the intermolecular association of succinoglycan entities rather than changes in intramolecular conformations. These results show that interpretation based on modeling is limited at this level and that a combination of several experimental techniques is necessarily required to gain an unambiguous understanding of the size, charge, and electrophoretic mobility of this complex macromolecule.

Acknowledgment. The authors acknowledge the Swiss National Science Foundation (V.S. PP002-102640, K.W. 200020-101788, and J.B. 200020-101974/1) for providing funding directly related to this work. Prof. M. Benedetti is thanked for performing the potentiometric titrations.

References and Notes

(1) Balnois, E.; Stoll, S.; Wilkinson, K. J.; Buffle, J. *Macromolecules* **2000**, *33*, 7440−7447.
(2) Boutebba, A.; Milas, M.; Rinaudo, M. *Int. J. Biol. Macromol.* **1999**, *24*, 319−327.
(3) Gravanis, G.; Milas, M.; Rinaudo, M.; Clarke-Sturman, A. J. *Int. J. Biol. Macromol.* **1990**, *12*, 195−200.
(4) Gravanis, G.; Milas, M.; Rinaudo, M. *Int. J. Biol. Macromol.* **1990**, *12*, 201−206.
(5) Boutebba, A.; Milas, M.; Rinaudo, M. *Biopolymers* **1997**, *42*, 811−819.
(6) Dentini, M.; Crescenzi, V.; Fidenza, M.; Coviello, T. *Macromolecules* **1989**, *22*, 954−959.
(7) Burovo, T. V.; Golubeva, I. A.; Grinberg, N. V.; Mashkevich, A. Y.; Grinberg, V. Y.; Usov, A. I.; Navarini, L.; Cesaro, A. *Biopolymers* **1996**, *39*, 517−529.
(8) Borsali, R.; Rinaudo, M.; Noirez, L. *Macromolecules* **1995**, *28*, 1085−1088.
(9) Lyklema, J. *Fundamentals of Interface and Colloid Science: Solid Liquid Interfaces*; Academic Press: London, 1995; Vol. II, Chapter 4.
(10) Ohshima, H. *Adv. Colloid Interface Sci.* **1995**, *62*, 189−235.
(11) Ohshima, H. *J. Colloid Interface Sci.* **2003**, *258*, 252−258.
(12) Duval, J. F. L.; Busscher, H. J.; van de Belt-Gritter, B.; van der Mei, H. C.; Norde, W. *Langmuir* **2005**, *21*, 11268−11282.
(13) Hill, R. J.; Saville, D. A.; Russel, W. B. *J. Colloid Interface Sci.* **2003**, *258*, 56−74.
(14) Duval, J. F. L.; Wilkinson, K. J.; van Leeuwen, H. P.; Buffle, J. *Environ. Sci. Technol.* **2005**, *39*, 6435−6445.
(15) Thompson, N. L. Fluorescence correlation spectroscopy. *Topics of fluorescence correlation spectroscopy*; Plenum Press: New York, 1991; Vol. 1.
(16) Magde, D.; Elson, E. L.; Webb, W. W. *Biopolymers* **1974**, *13* (1), 29−61.
(17) Meunier, F.; Wilkinson, K. J. *Biomacromolecules* **2002**, *3*, 857−864.
(18) Tinland, B.; Maret, G.; Rinaudo, M. *Macromolecules* **1990**, *23*, 596−602.
(19) Buffle, J. *Complexation reactions in aquatic systems*; Ellis Horwood, Chichester, U.K., 1988.
(20) Kirkwood, J. G.; Riseman, J. *J. Chem. Phys.* **1948**, *16*, 565−573.
(21) Yamakawa, H. *Macromolecules* **1977**, *10*, 692−696.
(22) Broersma, S. *J. Chem. Phys.* **1960**, *32*, 1626−1632.
(23) Harris, R. A.; Hearst, J. E. *J. Chem. Phys.* **1966**, *44*, 2595−2602;
(24) Harris, R. A.; Hearst, J. E. *J. Chem. Phys.* **1967**, *46*, 398.
(25) Schiewer, S.; Volesky, B. *Environ. Sci. Technol.* **1997**, *31* (7), 1863−1871.
(26) Deslandes, Y.; Marchessault, R. H.; Sarko, A. *Macromolecules* **1980**, *13*, 1466−1471.
(27) Duval, J. F. L.; van Leeuwen, H. P. *Langmuir* **2004**, *20*, 10324−10336.
(28) Duval, J. F. L. *Langmuir* **2005**, *21*, 3247−3258.
(29) Press, W. H.; Teukolsky, S. A.; Vetterling, W. T.; Flannery, B. P. *Numerical Recipes in Fortran, The art of Scientific Computing*, 2nd ed.; Cambridge University Press: New York, 1986.
(30) Duval, J. F. L.; Ohshima, H. *Langmuir* **2006**, *22*, 3533−3546.
(31) Ohshima, H. *Colloid Polym. Sci.* **2001**, *279*, 88−91.
(32) Keizer, A.; de van der Drift, W. P. J. T.; Overbeek, J. T. G. *Biophys. Chem.* **1975**, *3*, 107−108.
(33) Landau, L. D.; Lifshitz, E. M. *Fluid Mechanics*; Pergamon: London, 1966.
(34) Debye, P.; Bueche, A. *J. Chem. Phys.* **1948**, *16*, 573.
(35) Dautray, R.; Lions, J. L. *Analyse Mathématique et Calcul Numérique pour les Sciences et les Techniques*; Evolution Numérique: Transport, Edition Masson, 1988; Vol. 9.
(36) Fatin-Rouge, N.; Buffle, J. Study of environmental systems by means of Fluorescence Correlation Spectroscopy. In *Environmental colloids: behaviour, structure and characterisation*; Wilkinson, K. J., Lead, J. R., Eds.; Chichester, 2006 (in press).
(37) Benedetti, M. F.; Ranville, J. F.; Ponthieu, M.; Pinheiro J. P. *Org. Geochem.* **2002** *33*, 269−279.
(38) Benedetti, M. F.; van Riemsdijk, W. H.; Koopal, L. K. *Environ. Sci. Technol.* **1996**, *30*, 1805−1813.
(39) Hermans, J. J.; Fujita, H. *Koninkl. Ned. Akad. Wetenschapter Proc.* **1955**, *B58*, 182.
(40) Saville, D. A. *J. Colloid Interface Sci.* **2000**, *222*, 137.
(41) Kido, S.; Nakanishi, T.; Norisuye, T.; Kaneda, I.; Yanaki, T. *Biomacromolecules* **2001**, *2*, 952−957.

BM060346N